acta physica slovaca vol. 54 No. 2, 147 – 161 April 2004

ON STRUCTURAL PROPERTIES OF Si/Zr(Y)O_2 AND Zr(Y)O_2/Si SYSTEMS [1]

E. Pinčík[a2], M. Jergel[b3], J. Müllerová[c], C. Falcony[b], L. Ortega[d], A.N. Buzynin[e], E. Lomonova[e], R. Brunner[a], Š. Chromik[f], M. Hartmanová[a]

[a] *Institute of Physics, Slovak Academy of Sciences, Dúbravská cesta 9 SK-842 28 Bratislava, Slovakia*

[b] *Departmento de Física, CINVESTAV-IPN, Apdo. Postal 14-740 07300 México D.F., México*

[c] *Department of Physics, Faculty of Logistics, Military Academy SK-031 01 Liptovský Mikuláš, Slovakia*

[d] *Laboratoire de Cristallographie du CNRS, BP 166 38042 Grenoble Cedex 09, France*

[e] *General Physics Institute, Academy of Sciences, Moscow, Russia*

[f] *Institute of Electrical Engineering, Slovak Academy of Sciences Dúbravská cesta 9, 842 39 Bratislava, Slovakia*

Received 3 April 2003, accepted 16 July 2003

The paper deals with the formation of polycrystalline structure of deposited YSZ and Si films on Si and YSZ crystals, respectively, depending on the substrate surface orientation and with the evolution of the YSZ/Si interface properties at the initial stage of the plasma anodization. The X-ray measurements confirmed that YSZ film deposited on Si is amorphous or polycrystalline. A well developed face centered cubic (fcc) phase with lattice parameter of 0.509 nm is typical for the best YSZ layers, four intense 111, 200, 220 and 311 diffractions being usually detected. The polycrystalline structure of Si-on-YSZ layers was affected by the orientation of YSZ substrate surface, namely (100) or (111). The surface of crystalline silicon at the interface with deposited YSZ layer consisted of large polycrystalline blocks, their size being reduced by one order of magnitude after the plasma anodization. The YSZ/Si interface electrical properties were changed remarkably as found by DLTS which revealed a continuous spectrum of interface states originating due to the anodization. It is attributed to the formation of a very thin silicon oxide interlayer between the YSZ layer and Si crystal. The other electrical and optical properties were investigated by C-V, capacitance-frequency, deep level transient spectroscopy and reflectance spectroscopy.

PACS: 78.20.Ci, 78.66.Hf, 73.20.At, 52.75.Rx, 07.07.Df

[1]Presented at XIV$^{\rm th}$ Symposium on Application of Plasma Processes, Liptovský Mikuláš (Slovakia), January 2003.
[2]E-mail address: fyzipinc@savba.sk
[3]On the leave from the Institute of Physics SAS, Bratislava, Slovakia

0323-0465/04 © Institute of Physics, SAS, Bratislava, Slovakia

1 Introduction

A low-temperature ($< 600^\circ$ C) method of producing high-quality very thin dielectric layers of silicon is the subject of considerable research effort. The use of plasmas to grow such SiO_2 films on Si for electronic applications dates from the very early days of Si technology. Plasma oxidation is attractive as it offers a rapid growth of a silicon dioxide film of relatively high quality at the temperatures far below those required for conventional thermal oxidation. As a consequence, the dopant redistribution during the oxide growth is minimized and the generation of high-temperature-induced defects, as stacking faults, is reduced. Although recent research has shifted to producing chemical vapour depositied (CVD) oxides, the advantage of plasma oxidation is that silicon is consumed during the process as in thermal oxidation and therefore it is believed that plasma oxidation offers the best way of low temperature processing to provide nearly ideal thermally grown Si-SiO_2 interface.

The investigation of the $Zr(Y)O_2$ [usually labelled YSZ (yttrium stabilized zirconium)] thin layers is interesting because of two reasons. Firstly, the preparation of the $YBa_2Cu_3O_7$ superconducting thin films on Si where YSZ is used as a buffer layer [1,2]; secondly, the low-temperature SiO_2 growth by the plasma anodic oxidation process which can proceed if a relatively thick (~ 1 μm) ZrO_2 covering overlayer is deposited on the Si surface before oxidation [3]. The explanation of the latter effect is based on the idea that the negative oxygen ion conductivity of ZrO_2 layer is the dominant property determining the silicon oxide growth rate which is supposed to be very high. This contribution demonstrates different structural and optical properties of the YSZ/Si and Si/YSZ structures and clarifies the evolution of the YSZ ($\sim$100 nm)/ Si interface properties at the initial stage of the plasma anodozation when the silicon dioxide interlayer is considerable thin.

2 Sample preparation

The deposition of $\sim$ 100 nm thick YSZ layer on (100) oriented silicon substrate (n-type, 10^{16} cm^{-3}) was done by electron beam evaporation from the $Zr(Y)O_2$ target. The evaporation process is described in detail in the paper of Chromik et al [2]. The YSZ/Si structures were annealed at 930°C for 30 minutes. Plasma anodic oxidation of these samples was performed for 20 minutes after the deposition in the apparatus presented in the paper of Bartoš et al [4], the oxidation current density and sample temperature being 3.8 mAcm^{-3} and 250°C, respectively. Thin Si layers were deposited on the (100) and (111) crystalline YSZs by molecular beam epitaxy (MBE) technique.

3 Kinetic of the plasma oxidation

In this work, we have fitted the experimental growth curves (for 5, 10, and 20 mins oxidation time) for the anodic oxidation by assuming that the oxidation rate is limited by the rate of the ion transport through the oxide, i.e. by the rate at which the ions can move through the oxide layer under the assistance of the electric field. Only a little change of the field with the increase of the oxide thickness is supposed because the constant current mode of the growth was used. Verwey and Dewald [5] developed a discrete hopping model for ionic transport in high electric

fields, violating the Ohm‘s law relation. The essence was to consider the lowering of the discrete potential barrier for forward hopping of the ionic defects (interstitial vacancy). This approach was adopted by Cabrerra and Mott where the rate limited step was considered to be entry of metal ions into the oxide layer. Dewald [5] extended the model of Verwey to include the space charge of diffusing ionic species. The model was improved by Friedel [6] and Taylor [7]. In the hopping model, an electric field $E\left(x\right)$ lowers the potential energy barrier W by an amount $ZqEa$ where Zq is the charge of the particle and $2a$ is the separation distance between the adjacent energy minima. The field-modified activation energy for forward hopping will be thus $W - ZqEa$.

If ν is the single attempt-to-escape frequency of the charged particle back and forth in its potential well minimum and $n^{(f)}$ denotes the number of charged particles per unit area in planar slice of thickness $2a$, which is perpendicular to the hopping direction, and $n^{(r)}$ denotes the corresponding number located just beyond the same barrier, the number J of charged particles surmounting the barrier is the difference between forward and reverse hops over the barrier. Electric field raises the potential energy barrier by the amount $ZqEa$ in the reverse direction. J is thus given as

$$J = n^{(f)} \cdot \nu \cdot \exp \frac{-\left(W - ZqEa\right)}{kT} - n^{(r)} \cdot \nu \cdot \exp \frac{-\left(W + ZqEa\right)}{kT}. \quad (1)$$

If the concentration difference $n^{(f)} - n^{(r)}$ is supposed to be negligibly small, the equation (1) reduces to:

$$J \cong 2n^{(f)} \cdot \nu \cdot \exp \frac{-W}{kT} \cdot \sinh \frac{ZqEa}{kT}. \quad (2)$$

Supposing that the oxide/semiconductor interface reactions are very fast compared to the bulk migration, we can express the relation for the current density of single negatively charged oxygen ions, J_i, from the equations (1) and (2) in the form

$$J_i = Zq_i \frac{DC_0}{2a} g\left(d_{ox}\right) \exp\left(-\frac{U_{ox}}{d_{ox}E'} + 1\right), \quad (3)$$

where C_0 is the negative oxygen ion concentration on the oxide surface, D is the migration coefficient, Zq_i is the oxygen charge, $2a$ is the distance between two oxygen atoms in the oxide

$$E' = kT/q_i a, \quad (4)$$

and $g\left(d_{ox}\right)$ represents the reduction of the ionic current due to space charge:

$$g\left(d_{ox}\right) = \left(1 + d_{ox}/L'\right)^{-\left(1 + L'/d_{ox}\right)}, \quad (5)$$

where L' is the width of the space charge layer:

$$L' = \varepsilon\varepsilon_0 kT \Big/ \left(Zq_i\right)^2 aC_0. \quad (6)$$

By fitting procedure of relation (3), the values 5x10^{17} cm^{-3} and 2x10^{-11} cm^2s^{-1} of oxygen ion concentration, C_0, and migration coefficient, D, respectively, were obtained.

4 Experimental methods and results.

Three types of the samples were investigated by electrical methods [C-V, capacitance-frequency (C-f) and QDLTS]:

i) as grown polycrystalline layer YSZ on silicon (curve 1);

ii) YSZ/Si after the plasma anodic oxidation (curve 2) and

iii) ultrathin SiO_2/Si (curve 3).

i) C-V, capacitance-frequency (C-f) and charge version of deep level transient spectroscopy (Q-DLTS)

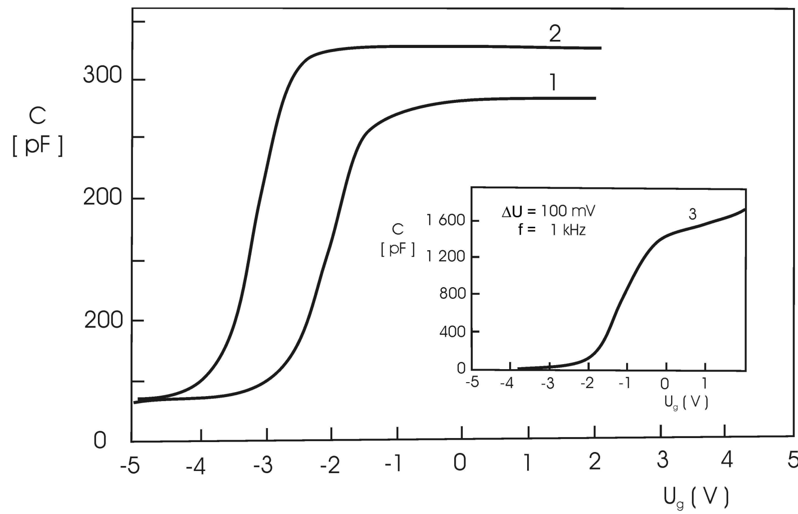

Fig. 1. C-V curves of YSZ / Si (1), plasma anodized YSZ / Si (2) and very thin SiO_2 / Si (3) structures. The last one is the initial stadium of high temperature YSZ growth on Si.

Deep level transient spectroscopy was performed by home-made equipment. As we have pointed out in [8] the large-signal excitation of the GaAs MOS diodes with the thin plasma oxide layer yields complicated signals which seriously makes any quantitative analysis difficult. For this reason, the present study is also restricted to small-signal charge deep level transient spectroscopy (Q-DLTS), the instrumentation being in principle identical with that developed by Farmer et al [9]. DLTS is often used to detect deep levels in the band gap of the semiconductors. We applied this type of measuring system to Al-ZrO_2-Si structures. The extremely high sensitivity of the Q-DLTS makes it possible to detect the response of the structures to the excitation by small gate voltages $\Delta U \sim kT/q$ or even less as a function of the dc bias U. The measurements were performed choosing repetition frequency of f_r = 40 Hz and rectangular excitation signal of amplitude ΔU = 50 mV. The preamplifier output signal was sampled at times t_1 = 0.5 ms

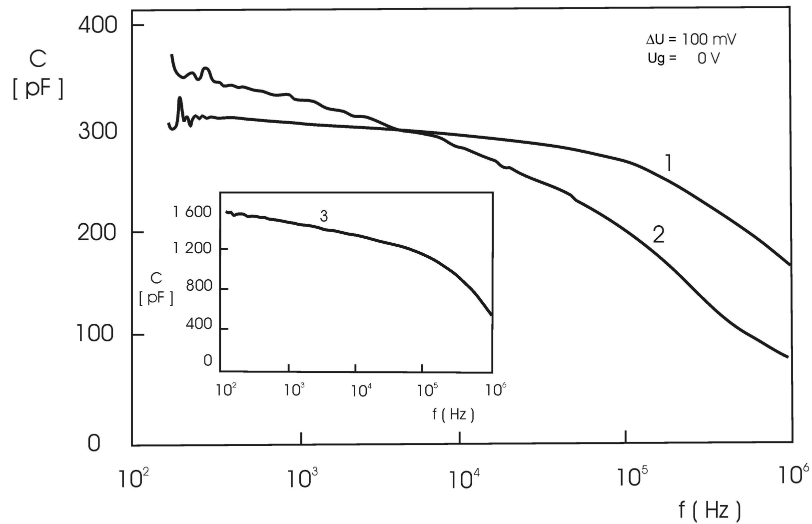

Fig. 2. Capacitance-frequency curves of YSZ / Si (1), plasma anodized YSZ / Si (2) and very thin SiO_2 / Si (3) structures.

and t_2 = 1 ms. The charge difference $\Delta Q = Q(t_1) - Q(t_2)$ was monitored with respect to the temperature T.

The YSZ/Si interface properties have dramaticaly changed due to the anodization as indicated by DLTS spectroscopy. The spectrum of virgin sample is characterized by only sharp single peak lying close to LN temperature and by a very low density of interface states. Continuous spectrum of the interface states has arised in the range of 100 K - 400 K after the low-temperature plasma anodization. It is attributed to the formation of thin ($\sim$10 nm) silicon oxide-like interlayer created under the influence of the high-intensive electric field used at anodization acting at extremely low temperature; and to the change of the flatband of the structure - see the C-f and C-V measurements of three types of the samples presented in Fig. 1 and Fig. 2, respectively.

C-V and C-f dependences were made using SOLARTRON SI 1260 impedance/gain phase analyser, interfaced to computer and run through a LAB-VIEW program. The impedance measurements vere made in the frequency range of 100 Hz – 1 MHz at temperature 493 K. Aluminium dots were evaporated onto the oxide layers through mask as the gate electrodes. Ohmic contact on the back side (crystalline Si) of the sandwich configuration were obtained by deposition of Au film. By this way we prepared MIS structure of the type Al-YSZ-Si-Au. C-V dependencies af above mentioned samples measured at 1 kHz are shown in Fig. 1. Frequence dependencies of corresponding capacitances are presented in Fig. 2. Measurements at 1 MHz confirmed that during the anodization the thickness of insulator (YSZ + underlaying anodically grown SiO_2) increased. The SiO_2 growth rate corresponds approximately 0.5 nm/min. (10 nm/20 min.) only. C-f dependences confirmed strong mobility of ions inbuilt in the formed dielectric. This fact is more evident after anodization procedure. It leads to such situation that at about 100 Hz the capacitances before and after anodization exchange their relative positions on

capacitance scale. We suppose that the ion conductivity properties of YSZ layers were considerably changed. The X-ray measurements indicated that the interface between YSZ and crystalline silicon has been amorphised and polycrystalline YSZ structure has been partly destroyed (size of polycrystalline blocks was reduced).

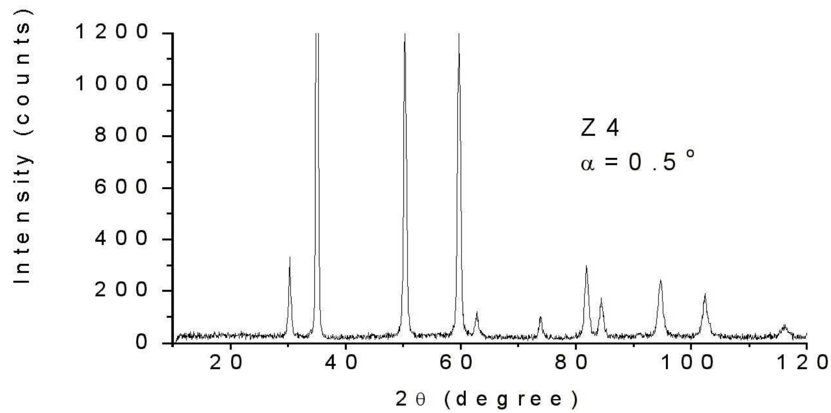

Fig. 3. XRDGI pattern measured on polycrystalline YSZ / Si structure at grazing incidence angle α=0.5 °.

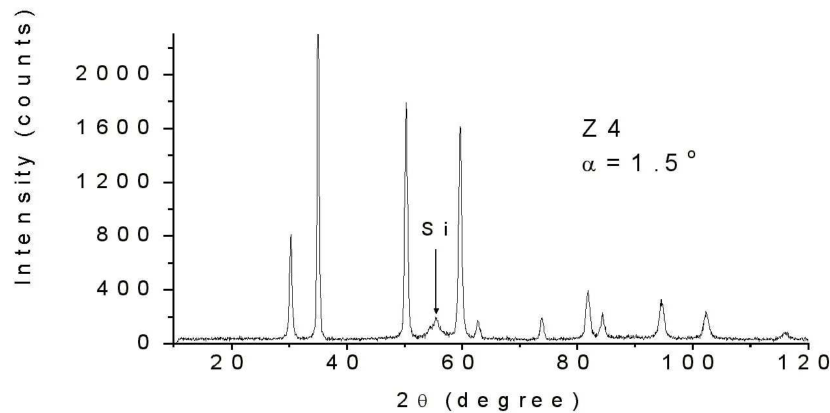

Fig. 4. XRDGI pattern measured on polycrystalline YSZ / Si structure at grazing incidence angle α=1.5 °.

The inserted graph in Fig. 2 (line No. 3) confirmed that also at the beginning stadium of YSZ formation the strong frequency dependence of capacitance of MIS structure is observed. Unfortunately, we do not have AES or SIMS analysis, but C-f dependence indicates that very thin YSZ layer was formed already. X-ray analysis (see Fig. 7, in comparison with Fig. 6) confirmed its amorphous structure.

ii) X-ray diffraction at grazing incidence (XRDGI)

We supposed that anodization process should be strongly influenced by structure of deposited YSZ layer. In another words, the kinetics will be controlled by number defect sites in the YSZ. Therefore we had to check the structural state of YSZ layers. It was measured on the 12 kW rotating anode RIGAKU generator with the CuKα radiation. The basic grazing angles were set to 0.5 ° and 1.5 °. We have analyzed two dominant structurally different YSZ layers, namely that one with polycrystalline structure (Figs. 3, 4) and the amorphous YSZ layer which is shown in Figs. 5, 6. The shape of the diffraction peak at $2\Theta = 56.1$ ° defines the structural properties of the crystalline silicon on which the YSZ was evaporated. This well known reflection comes from 311 Si plane. The X-ray diffraction pattern of the structure of very thin SiO_2 / Si is illustrated in Fig. 7.

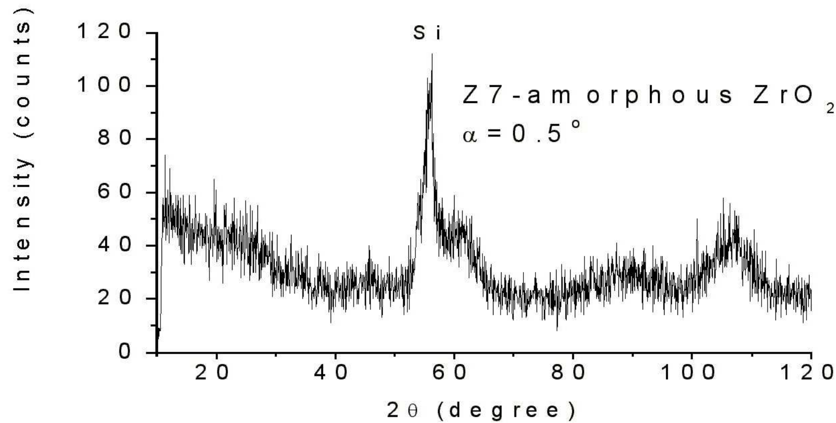

Fig. 5. XRDGI pattern measured on amorphous YSZ / Si structure at grazing incidence angle α=0.5 °.

Figs. 3-7 confirmed that little changes in YSZ deposition technology lead to different structure of the layer. We can prepare polycrystalline or amorphous type. For anodization experiments were choosen the YSZ layers with polycrystalline structure. The same type of the structure was used for reflectance measurements. All diffraction patterns illustrated in Figs. 37 belongs to tabelled patterns of YSZ (see e.g. Powder Diffraction Database (PDF-2) of JCPDS-ICDD diffraction data, International Center for Diffraction Data, Newton Square, PA, www.icdd.com).

The structure of YSZ layer is predefined by more parameters – at least by temperature of the substrate (crystalline Si), deposition growth rate, and by crystalline orientation of the used substrate. The last fact was verified at the growth of Si films on 100 and 111 YSZ surfaces.

In Figs. 8 and 9, diffraction patterns of thin Si films deposited by MBE technique on (100) and (111) oriented YSZ crystals are shown. The better development of polycrystalline structure was evidently observed on Si / YSZ (111) structures.

iii) Spectral reflectance

We have performed also the spectral reflectance measurements with the dominant aim to determine packing density of polycrystalline YSZ layers. This parameter cannot be investigated by electrical or X-ray techniques. Packing density can strongly influence kinetics of anodically

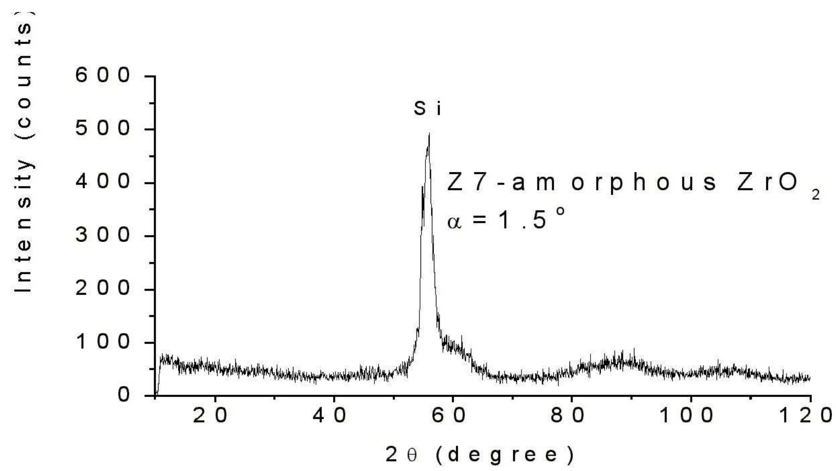

Fig. 6. XRDGI pattern measured on amorphous YSZ / Si structure at grazing incidence angle α=1.5 ° .

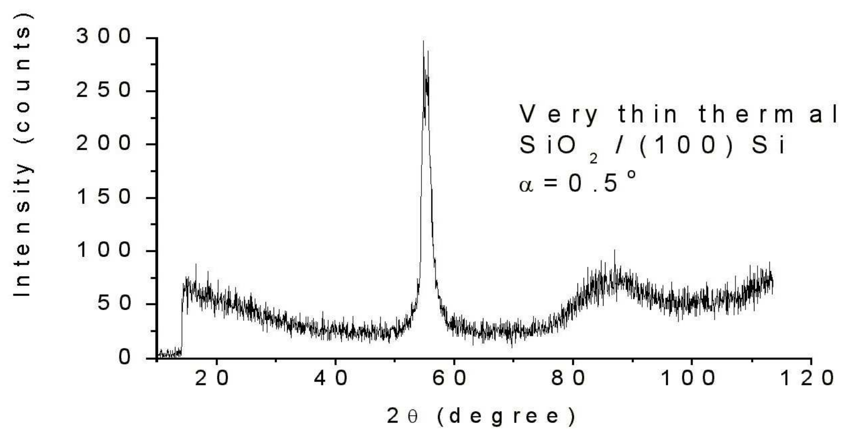

Fig. 7. XRDGI pattern measured on very thin SiO_2 / Si structure at grazing incidence angle α=0.5 ° . (The initial stadium of high temperature YSZ growth on Si).

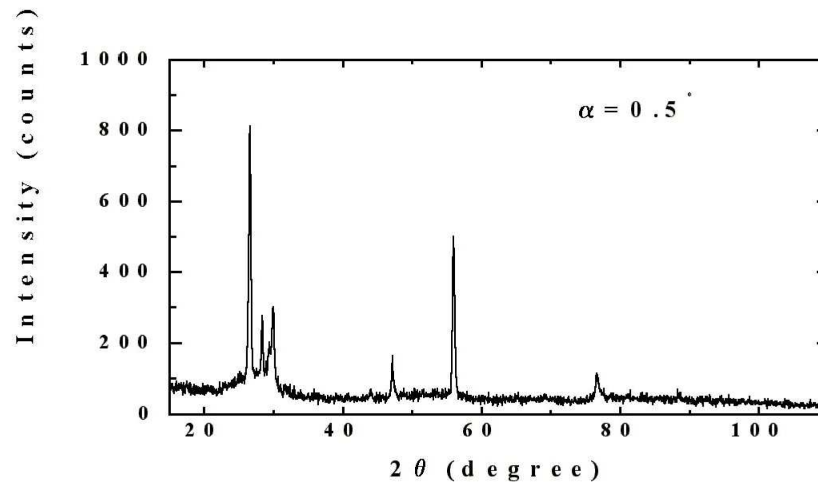

Fig. 8. XRDGI diffraction pattern of thin Si films deposited by MBE technique on (100) oriented YSZ crystals at grazing incidence angle α=0.5 $^\circ$.

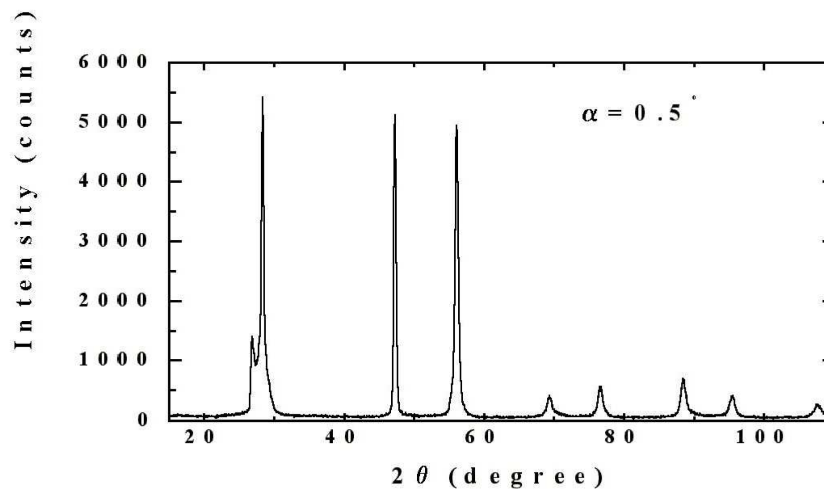

Fig. 9. XRDGI diffraction pattern of thin Si films deposited by MBE technique on (111) oriented YSZ crystals at grazing incidence angle α=0.5 $^\circ$. The better development of polycrystalline structure in comparison with Fig. 8 was evidently observed on Si(111) / YSZ structures.

grown SiO_2 laying underneath YSZ. Used optical method and corresponding original evaluation enable to estimate the number of dry voids and the number of voids totally filled with water.

Reflectance measurements were carried out by a double–beam Carl Zeiss Jena spectrophotometer Specord M40 with the slit of 2.5 nm at room temperature. An accessory for absolute reflectance measurement at nearly normal incidence was used with a freshly evaporated aluminium sample in the reference beam and special care was taken to provide the reproducibility of measurements. The values of $n_2,\ k_2$ were taken from [10] and confirmed by the Kramers–Kronig dispersion analysis of Si substrate reflectance spectrum. No significant differences were found between the reflection spectra from different areas of the samples. As the probed area was ~ 0.2 cm^2, the films can be considered homogeneous at least down to this scale. We have used an original theoretical approach for the evaluation of the reflectance spectra which we describe in more detaily.

5 Interference reflection spectrophotometry

The refractive index, extinction coefficient as well as the thickness of the film can be found by a transmittance $T(\lambda)$ or a reflectance $R(\lambda)$ spectrum of the film deposited on a transparent substrate. When the film is deposited on thick absorbing substrate, only spectral reflectance measurement is possible.

A thin isotropic film with the average thickness d is characterised by the complex refractive index $n_1 = (n_1 - i\,k_1)$ and the substrate (with the thickness $\gg d$) by the complex refractive index $n_2 = (n_2 - i\,k_2)$ where n_1 (n_2) is the real part of the complex refractive index and k_1 (k_2) is the imaginary part or the extinction coefficient. The optical reflectance of a parallel–sided thin isotropic homogeneous film on a thick partly absorbing substrate, both immersed in air, is given as

$$R = \frac{A + Bx + Cx^2}{D + Ex + Fx^2} \tag{7}$$

where $x = \exp(-\alpha d)$ is the absorbance, $\alpha = (4\pi k_1)/\lambda$is the absorption coefficient, $\Phi = (4\pi n_1 d)/\lambda$,

$$\begin{aligned}
A &= \left[(1-n_1)^2 + k_1^2\right]\left[(n_1+n_2)^2 + (k_1+k_2)^2\right] ,\\
C &= \left[(1+n_1)^2 + k_1^2\right]\left[(n_1-n_2)^2 + (k_1-k_2)^2\right] ,\\
D &= \left[(1+n_1)^2 + k_1^2\right]\left[(n_1+n_2)^2 + (k_1+k_2)^2\right] ,\\
F &= \left[(1-n_1)^2 + k_1^2\right]\left[(n_1-n_2)^2 + (k_1-k_2)^2\right] ,\\
B &= 2\left[A'\cos\Phi + B'\sin\Phi\right],\ E = 2\left[C'\cos\Phi + D'\sin\Phi\right] ,\\
A' &= \left(1-n_1^2-k_1^2\right)\left(n_1^2-n_2^2+k_1^2-k_2^2\right) + 4k_1\left(n_1k_2-n_2k_1\right) ,\\
B' &= \left(1-n_1^2-k_1^2\right)\left(n_1k_2-n_2k_1\right) - 2k_1\left(n_1^2-n_2^2+k_1^2-k_2^2\right) ,\\
C' &= \left(1-n_1^2-k_1^2\right)\left(n_1^2-n_2^2+k_1^2-k_2^2\right) - 4k_1\left(n_1k_2-n_2k_1\right) ,\\
D' &= \left(1-n_1^2-k_1^2\right)\left(n_1k_2-n_2k_1\right) + 2k_1\left(n_1^2-n_2^2+k_1^2-k_2^2\right) .
\end{aligned} \tag{8}$$

Since the equation is not reversible, a fitting procedure is necessary to calculate $n_1, k_1, d$and to get the best fit between the measured reflectance $R_{\rm exp}$ and the calculated value R. The calculated reflectance $R(\lambda_i, n_i, k_1, d)$is the function of three parameters n_1, k_1, d according to

Eqs. (7), (8) and can be fitted to the measured reflectance $R_{\rm exp}$by several approaches such as least square $\sum_i \left[R_{\rm exp}\left(\lambda\right) - R\left(\lambda_i, n_1, k_1, d\right)\right]^2$minimisation and looking for a global minimum or local minima for each parameter.

6 Envelope method

In the interference spectrophotometry, especially in the transmittance mode, the envelope method is often used [11, 12]. Obviously, only one independent parameter can be determined from a single reflectance measurement. When the film is slightly absorbing, interference effects coming from multiple coherent reflections at the interfaces are present in the reflectance spectrum and the above mentioned parameters can be determined from the envelopes $R_{\rm max}$ and $R_{\rm min}$along the interference maxima and minima. A widely used version of the envelope method has been developed by Swanepoel [11] for transmittance measurement. The versions based on the reflectance alone are seldom [13].

The reflectance R can be expressed for the envelopes of the interference fringes using the conditions for the interference maxima $2n_1 d = m\lambda$ and the interference minima $2n_1 d = \left(2m+1\right)\lambda/2, \quad |m| = 0,\, 1,\, 2\ldots$ Hence, the envelopes of the interference maxima $R_{\rm max}$ and interference minima $R_{\rm min}$ are given by Eq. (7) with the parameters A, C, D, F according to Eq. (8) but with the following parameters (for $n_1 < n_2$) for $R_{\rm max}$

$$\begin{aligned} B &= 2\left[\left(1-n_1^2-k_1^2\right)\left(n_1^2-n_2^2+k_1^2-k_2^2\right)+4k_1\left(n_1k_2-n_2k_1\right)\right]\,, \\ E &= 2\left[\left(1-n_1^2-k_1^2\right)\left(n_1^2-n_2^2+k_1^2-k_2^2\right)-4k_1\left(n_1k_2-n_2k_1\right)\right] \end{aligned}$$

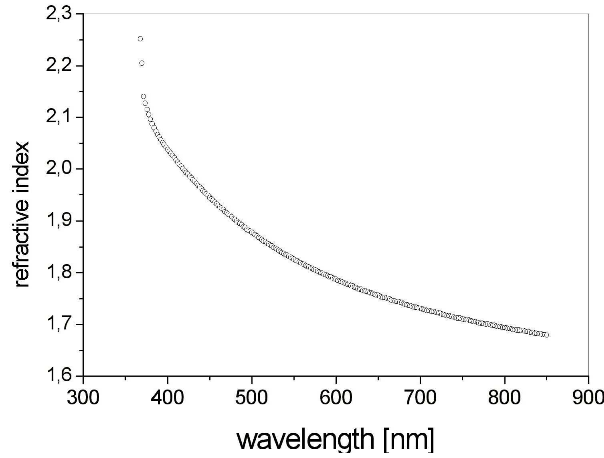

Fig. 10. Dispersion of real part of complex refractive index of polycrystalline YSZ layer deposited on Si. The measurement was performed on sample already characterized on Figs. 3, 4.

and for $R_{\rm min}$

$$\begin{aligned} B &= 2\left[\left(1-n_1^2-k_1^2\right)\left(n_1^2-n_2^2+k_1^2-k_2^2\right)+4k_1\left(n_1k_2-n_2k_1\right)\right]\,, \\ E &= -2\left[\left(1-n_1^2-k_1^2\right)\left(n_1^2-n_2^2+k_1^2-k_2^2\right)-4k_1\left(n_1k_2-n_2k_1\right)\right]\,. \end{aligned} \tag{9}$$

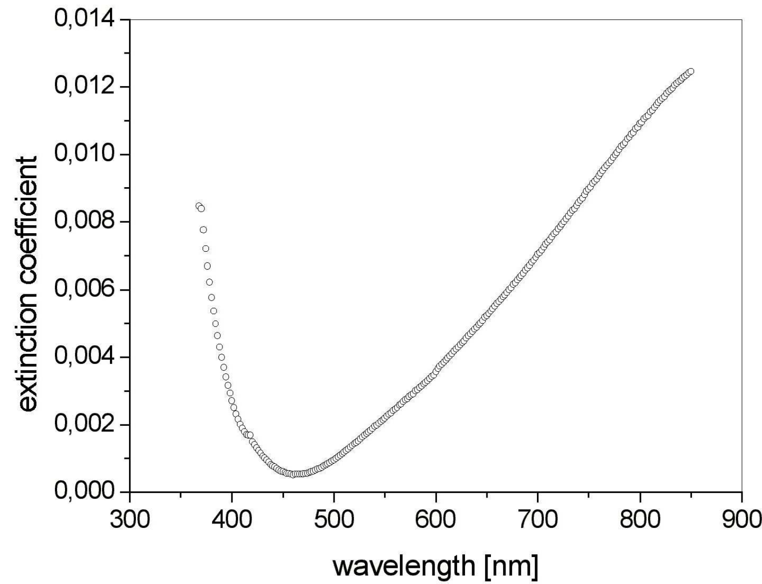

Fig. 11. Dispersion of extinction coefficient of the same polycrystalline YSZ layer as in Fig. 10.

Equations for $R_{\max}$, $R_{\min}$ are non–linear equations of n_1, k_1. Expressing x from $R_{\max}$, $R_{\min}$ and equating them, a polynomial for independent parameters n_1, k_1 is obtained at each wavelength. The optical parameters $n_1,\ k_1$ are determined numerically in several steps.

In the reflectance spectrum with the interference fringes, the assumption $n_1^2 \gg k_1^2$ is valid. Assuming this in the polynomial obtained from $R_{\max}$, $R_{\min}$, we minimize numerically the residuum $\sum_i \left[R_{\exp}(\lambda) - R(\lambda_i, n_1, k_1, d)\right]^2$ for n_1 and the initial value of k_1. Assuming $R_{\max}$, $R_{\min}$ to be continuous functions of the wavelength, $n_1,\ k_1$ as the functions of λ can be obtained. The initial value of k_1 is used in the recalculation of $n_1,\ k_1$ according to the above described procedure without the assumption $n_1^2 \gg k_1^2$. The procedure of successive iterations is repeated until the satisfactory accuracy in $n_1,\ k_1$is obtained. Knowing n_1 as the function of λ, we calculate the thickness d according to the standard equation for two adjacent interference fringes at wavelengths λ_m, λ_n: $d = \frac{\lambda_m \lambda_n}{2(\lambda_m n_n - \lambda_n n_m)}$ (n_m, n_n are refractive indices corresponding to these wavelengths).

The results of theoretical analysis of the experimental reflectance data obtained on YSZ/Si (sample Z4 see Figs. 3, 4) are illustrated as dependencies $n(\lambda)$, $k(\lambda)$ and $R(\lambda)$ in Figs. 10, 11, and 12, respectively.

Experimental reflectance and reflectance spectrum retrieved from determined n, k differ to some extent in position of interference extrema which may be caused by the film inhomogeneity. Thermally evaporated ZrO_2 or ZrO_2-Y_2O_3 (YSZ) films are often reported to be optically inhomogeneous [14] with columnar structure. Column diameters depend on the deposition conditions and the distance from the substrate surface and with the pores (voids) between the columns filled with water or being dry. The ratio of the volume of solid part of the film to the total volume of the film including voids is called the packing density p which is a worthy characteristic of the

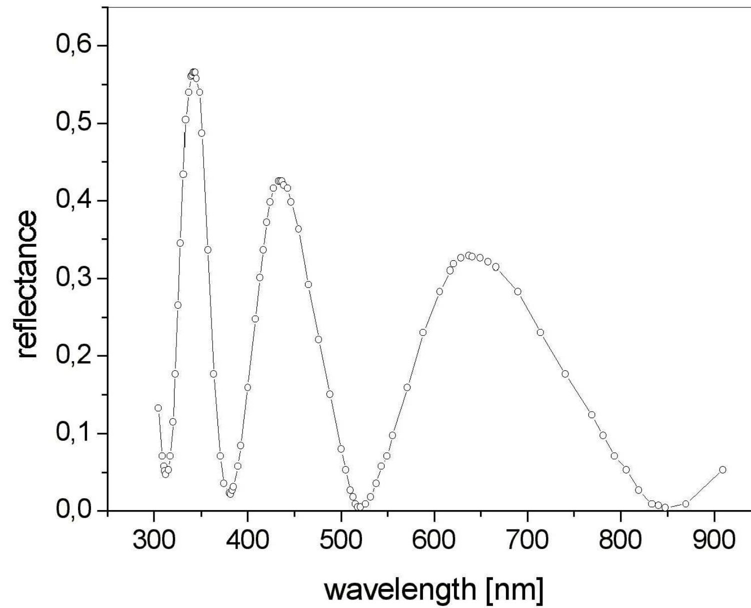

Fig. 12. Experimental reflectance spectrum of the same polycrystalline YSZ layer as in Fig. 10.

film.

As the packing density can be estimated using the value of the refractive index of the film, it expresses the correlation between structural and optical properties of the films. Higher values of the refractive index correspond to more densificated films.

Following the Bragg and Pippard model [14], the packing density p can be expresses by the equation

$$p = \frac{(n_c^2 + n_v^2)(n^2 - n_v^2)}{(n_c^2 - n_v^2)(n^2 + n_v^2)} \tag{10}$$

where n_c is the refractive index of columns at one specific wavelength, n_v is the refractive index of voids (voids filled with water n_v = 1.33, dry voids n_v = 1). The dependence p(n) is in Fig. 13 for $n_c \approx 2.16$ at 590 nm corresponding columns equal to bulk YSZ [15].

For sample under study the optical inhomogeneity influenced the optical characterization received by the envelope method. Final values of refractive index must be taken as average because of the assumption of the homogeneity of the film in the envelope method of processing the experimental data. No conclusions were made concerning the influence of the thickness variation of the samples on their optical properties.

For the corresponding thin film refractive index value n = 1.79 at 590 nm the following packing density was found assuming dry voids $p \sim 0.82$. Assuming voids filled with water $p \sim 0.65$. Therefore either voids are dry either they are partly occupied by water, which is more likely. The water content in porous films may be confirmed by additional infrared spectra measurements.

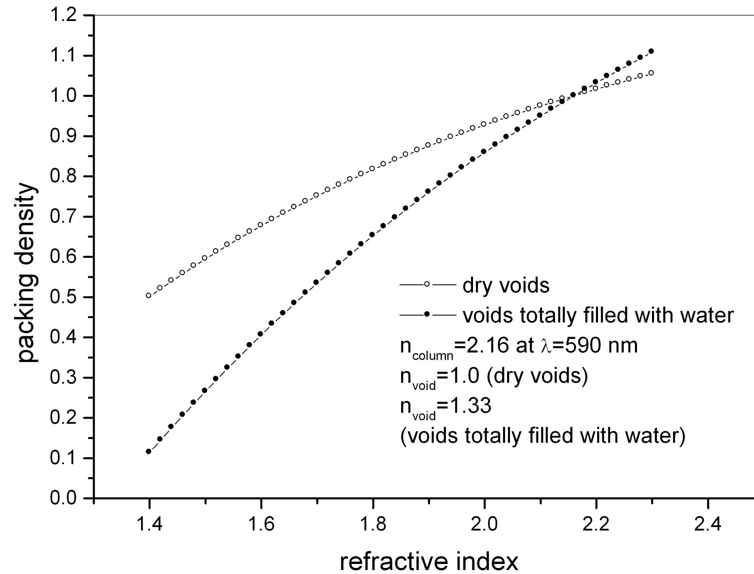

Fig. 13. The packing density versus refractive index of the film with dry voids or voids filled with water.

In this paragraph we have shown that befor any plasma treatment of YSZ layers they must be checked e.g. by optical reflectance method to obtain basic information on such properties as refractive index, extinction coefficient, packing density,... They all considerably influence plasma treatment process.

7 Conclusions

The XRD measurements confirmed that the deposited YSZ overlayer can have polycrystalline or amorphous character. Our polycrystalline YSZ layers have very well developed face centered cubic (fcc) phase with the lattice parameter $a = 0.509$ nm determined from the 200 peak. The average grain size D = 16.8 nm was determined.

Silicon at the interface with YSZ consists of large polycrystalline blocks. The size of these blocks was reduced by one order during the plasma anodization procedure, which could be characterized by the values 5×10^{17} cm^{-3} and 2×10^{-11} cm^{2}s^{-1} of oxygen ion concentration, C_0, and migration coefficient, D, respectively.

The YSZ/Si interface properties have dramaticaly changed due to the anodization as indicated by DLTS spectroscopy,. The spectrum of virgin sample is characterized by only sharp single peak lying close to LN temperature and by a very low density of interface states. Continuous spectrum of the interface states has arised in the range of 100 K - 400 K after the low-temperature plasma anodization. It is attributed to the formation of thin silicon oxide-like interlayer created under the influence of the high-intensive electric field used at anodization acting at extremely low temperature; and to the change of the flatband of the structure.

The observed growth rate of the oxide interlayer ($\sim$ 10 nm per 20 minutes) is smaller than

that presented by Periere et al [16]. We suppose that the high ordered polycrystalline YSZ thin virgin layer contains very low density of oxygen vacancies which are inevitable for a remarkable negative oxygen migration and therefore the plasma anodization flow measured by electrical methods consists mainly of electrons.

For the corresponding thin polycrystalline YSZ film (sample Z4), as it was used in anodization experiments, refractive index value n = 1.79 at 590 nm the following packing density was found assuming dry voids $p \sim 0.82$.

We have shown that before anodization procedure is necessary to check carefully electrical, structural and optical properties of deposited layers to be able to evaluate plasma interaction process.

Acknowledgement: The support of the Slovak grant agency VEGA 2/1119/22 is acknowledged.

References

[1] A. Lubig, C. Buchal, J. Schubert, C. Copeli, D. Guggi, L. Jia, B. Stritzker: *J. Appl. Phys.* **71** (1992) 5560

[2] Š. Chromik, B. Wuyts, I. Vávra, H. Rosová, F. Hanic, Š. Beňačka, Y. Bruynseraedo: *Physica C* **226** (1994) 153 ; M. Hartmanová, I. Thurzo, M. Jergel, J. Bartoš, F. Kadlec, V. Zelezný, D. Tunega, F. Kundracik, Š. Chromik. M. Brunel: *J. of Materials Science* **33** (1998) 969

[3] J. Perriere, B. Pelloie, J. Siejka: *Philosophical Magazine B* **55** (1987) 271

[4] J. Bartoš, E. Pinčík: *Thin Solid Films* **247** (1994) 178

[5] J.F. Dewald: *J. Electrochem. Soc.* **102** (1955) 1

[6] P. Friedel, S. Gourrier, P. Dimitriou: *J. Electrochem. Soc.* **128** (1981) 1857

[7] S. Taylor, W. Eccleston, K.J. Barlow: *J. Appl. Phys.* **64** (1988) 6515

[8] I. Thurzo, E. Pinčík: *Phys. Stat. Sol (a)* **86** (1984) 795

[9] J.W. Farmer, C.D. Lamb, J.M. Meese: *Appl. Phys. Lett.* **41** (1982) 1063

[10] V.I. Gavrilenko, A.M. Grechov, D.V. Korbutjak, V.G. Litovchenko: *Optical parameters of semiconductors*, Naukovaja dumka, Kiev, 1978, (in Russian)

[11] D. Minkov, R. Swanepoel: *Optical Engineering* **32** (1993) 3333

[12] M. Nenkov, T. Pencheva: *J. Opt. Soc. Am.* **15** (1998) 1852

[13] J.M. Gonzalez-Leal, E. Marquez, A.M. Bernal-Oliva, J.J. Ruiz-Perez, R. Jimenez-Garay: *Thin Solid Films* **317** (1998) 223

[14] M. Boulouz et al.: *Thin Solid Films* **323** (1998) 85

[15] V. M. Zolotarev, V. N. Morozov, E. V. Smirnova: *Optical Constants of Natural and Technological Materials*, Chimija, Leningrad 1984 (in Russian)

[16] J. Perriere, J. Siejka, R.P.H. Chang: *J. Appl. Phys.* **56** (1984) 2716